

“Cooling by heating” – demonstrating the significance of the longitudinal specific heat

Jon J. Papini, Jeppe C. Dyre, and Tage Christensen*
DNRF Centre “Glass and Time”, IMFUFA, Department of Sciences,
Roskilde University, Postbox 260, DK-4000 Roskilde, Denmark
(Dated: August 26, 2021)

Heating a solid sphere at the surface induces mechanical stresses inside the sphere. If a finite amount of heat is supplied, the stresses gradually disappear as temperature becomes homogeneous throughout the sphere. We show that before this happens, there is a temporary lowering of pressure and density in the interior of the sphere, inducing a transient lowering of the temperature here. For ordinary solids this effect is small because $c_p \cong c_V$. For fluent liquids the effect is negligible because their dynamic shear modulus vanishes. For a liquid at its glass transition, however, the effect is generally considerably larger than in solids. This paper presents analytical solutions of the relevant coupled thermoviscoelastic equations. In general, there is a difference between the isobaric specific heat, c_p , measured at constant isotropic pressure and the longitudinal specific heat, c_l , pertaining to mechanical boundary conditions that confine the associated expansion to be longitudinal. In the exact treatment of heat propagation the heat diffusion constant contains c_l rather than c_p . We show that the key parameter controlling the magnitude of the “cooling-by-heating” effect is the relative difference between these two specific heats. For a typical glass-forming liquid, when temperature at the surface is increased by 1 K, a lowering of the temperature in the sphere center of order 5 mK is expected if the experiment is performed at the glass transition. The cooling-by-heating effect is confirmed by measurements on a 19 mm diameter glucose sphere at the glass transition.

PACS numbers:

I. INTRODUCTION

Most solids and liquids expand when heated. Heat diffusion is a notoriously slow process, and heating a solid sample at its surface induces stresses in the sample that only disappear when temperature gradually becomes again homogeneous throughout. Heating a lightly fluent fluid that has a free surface (i.e., is free to expand), on the other hand, makes the entire sample expand on the time scale set by the sound velocity and sample dimensions. In this case there are no transient stresses beyond the acoustic time scale. A liquid close to its glass transition provides an interesting case in between solid and fluid behavior. Such a liquid behaves like a solid on time scales shorter than the Maxwell relaxation time $\tau_M = \eta/G_\infty$ where η is the shear viscosity and G_∞ the instantaneous shear modulus. The Maxwell relaxation time becomes longer than one second when a liquid approaches its calorimetric glass transition, implying that induced stresses survive for seconds or more.

This paper discusses the “cooling-by-heating” effect that arises when a sample is heated at a free surface. We show that this effect, which is present in all hard solids with a non-zero thermal expansion coefficient, is generally magnified considerably for glass-forming liquids close to their glass-transition temperature T_g . This is because close to T_g the liquid is solid-like by having a large, non-zero dynamic shear modulus on short time scales and, at the same time, is liquid-like by having a fairly large thermal expansion coefficient.

Returning to the case of a solid, what happens when heat is supplied at the (free) surface of a spherical sample? The outermost layers *attempt* to expand, obviously, but *a priori* one may imagine two different possibilities: 1) the expansion presses inwards, resulting in an increase of the pressure at the center of the sphere; or: 2) the expansion turns outwards, thus transmitting a negative pressure into the sphere. Which of the two possibilities that applies is answered by the application of standard thermoelasticity theory to the problem of calculating the stresses induced by the heating. This is done in the present paper. It turns out that case 2 applies—the sphere expands and pressure decreases in the interior of the sphere. This induces an adiabatic cooling inside the sphere. The phenomenon of cooling caused by heating at the surface is referred to below as the cooling-by-heating effect.

The solution of the coupled thermomechanical equations detailed in Sec. III shows that the cooling-by-heating effect is proportional to the difference between the reciprocals of the isobaric specific heat, c_p and the longitudinal specific heat, c_l (all specific heats are per unit volume); the latter quantity was introduced and discussed in Refs. 1, 2. The longitudinal specific heat

*Electronic address: tec@ruc.dk

is related to the isochoric specific heat, c_V , by

$$c_l = \frac{M_S}{M_T} c_V, \quad (1)$$

where M_S and M_T are the adiabatic and isothermal longitudinal moduli respectively. This is analogous to the standard thermodynamic relation $c_p = (K_S/K_T)c_V$ relating the isobaric specific heat to the isochoric specific heats in terms of the adiabatic, K_S and isothermal, K_T bulk moduli. Since $M_S = K_S + (4/3)G$ and $M_T = K_T + (4/3)G$, where G is shear modulus, one readily finds that c_l is in between c_V and c_p . As we shall see, the relative difference $a_l = (c_p - c_l)/c_p$ controls the strength of the cooling-by-heating effect, and we thus term this quantity the ‘‘longitudinal thermomechanical coupling constant’’. Combining the equations above a_l is found to be the product of two factors [1],

$$a_l \equiv \frac{c_p - c_l}{c_p} = \frac{4}{3} \frac{G}{M_T} \frac{c_p - c_V}{c_p}. \quad (2)$$

The first factor shows that there is only cooling by heating if the shear modulus is non-vanishing compared to the longitudinal modulus. The other factor, ‘‘the thermomechanical coupling’’, $a = (c_p - c_V)/c_p$ is a dimensionless measure of the coupling between thermal and mechanical perturbations. It can be expressed in terms of the expansivity, $\alpha_p \equiv (1/V)(\partial V/\partial T)_p$, as follows:

$$a \equiv \frac{c_p - c_V}{c_p} = \frac{T_0 \alpha_p^2 K_T}{c_p}, \quad (3)$$

where T_0 is the temperature. It follows that the cooling-by-heating effect is quadratic in the thermal expansion coefficient α_p .

Since solids typically expand significantly less upon heating than do liquids, the cooling-by-heating effect is generally small in solids. As an example, for solid glucose the thermal expansion coefficient [3] is $1.1 \cdot 10^{-4} \text{ K}^{-1}$ close to the glass transition whereas for liquid glucose it is $3.7 \cdot 10^{-4} \text{ K}^{-1}$ in the same temperature region. This potentially enhances the cooling-by-heating effect by a factor of 11. However the changes in c_p [3] from $1.91 \cdot 10^6 \text{ JK}^{-1}\text{m}^{-3}$ to $3.05 \cdot 10^6 \text{ JK}^{-1}\text{m}^{-3}$ and in K_T [4] from $10.75 \cdot 10^9 \text{ Pa}$ to $6.49 \cdot 10^9 \text{ Pa}$ reduces this to a factor of 8. Here we have used a density of $1.52 \cdot 10^3 \text{ kg m}^{-3}$ to convert specific heat data from mass to volume. It is, however, not unusual for liquid expansivities to be near 10^{-3} K^{-1} for which we would expect an enhancement of the thermomechanical coupling $a = (c_p - c_V)/c_p$ by a factor of 30. The shear modulus of glucose in the glassy state is $G_\infty = 3.1 \cdot 10^9 \text{ Pa}$ as deduced from the shear compliance data of Meyer and Ferry [5].

The above relations all generalize to deal with complex, frequency-dependent (dynamic) specific heats and moduli and expansivity, which are the relevant quantities when studying glass-forming liquids. Near the glass transition the cooling-by-heating effect may be studied on second time scales. Here, upon increasing the frequency, the factor G/M_T of Eq. (2) increases while at the same time the factor $(c_p - c_V)/c_p$ decreases. The enhancement of the cooling-by-heating effect is thus critically dependent on the relative time scales of the different relaxation processes at the glass transition. If the shear stress relaxes faster than the the volume processes, the cooling-by-heating effect may not be pronounced. This situation is illustrated in Fig. 1. The model describing the relaxation behavior between high- and low-frequency values is described in section IV.

The present work discusses the basis of cooling by heating by referring to the equations of standard linear thermoviscoelasticity. Section II introduces the general framework of thermoelasticity and thermoviscoelasticity. It is shown that the heat diffusion constant involves the longitudinal specific heat. Section III discusses the case when a finite amount of heat is fed into a sample at its surface at $t = 0$, as well as the experimentally easier realized case when temperature is suddenly increased at the surface. That section also presents analytical calculations of the ordinary solid case for which the constitutive properties do not undergo relaxation. Section IV gives calculations of a model glass-forming liquid, i.e., the case when the constitutive properties are frequency dependent. We estimate the effect to be of order 5 mK in the center of a sphere for a temperature increase at the sphere surface of one Kelvin. Section V confirms this prediction for measurements on a glucose sphere. Sections VI and VII briefly discuss and summarize the paper.

II. THERMOELASTICITY AND HEAT DIFFUSION.

Thermoelasticity deals with problems where displacement field $\mathbf{u}(\mathbf{r}, t)$ and temperature field $T(\mathbf{r}, t)$ couple. It is a linear theory of small deformations given in terms of the strain tensor $\epsilon_{ij} = \frac{1}{2}(\frac{\partial u_i}{\partial x_j} + \frac{\partial u_j}{\partial x_i})$ and small temperature increments $\delta T = T - T_0$ relative to a reference temperature T_0 . The material properties of a thermoelastic medium is given by the linear constitutive equations that expresses stress σ_{ij} and increments in entropy density δs in terms of ϵ_{ij} and δT . The hydrostatic pressure is related to the trace of the stress tensor $p = -1/3 \sum_i \sigma_{ii}$ and the relative compression is the trace of the strain tensor $\epsilon = \sum_i \epsilon_{ii} = \nabla \cdot \mathbf{u}$. The following constitutive equations [6] define the shear modulus G , the isothermal bulk modulus, K_T , the isochoric specific

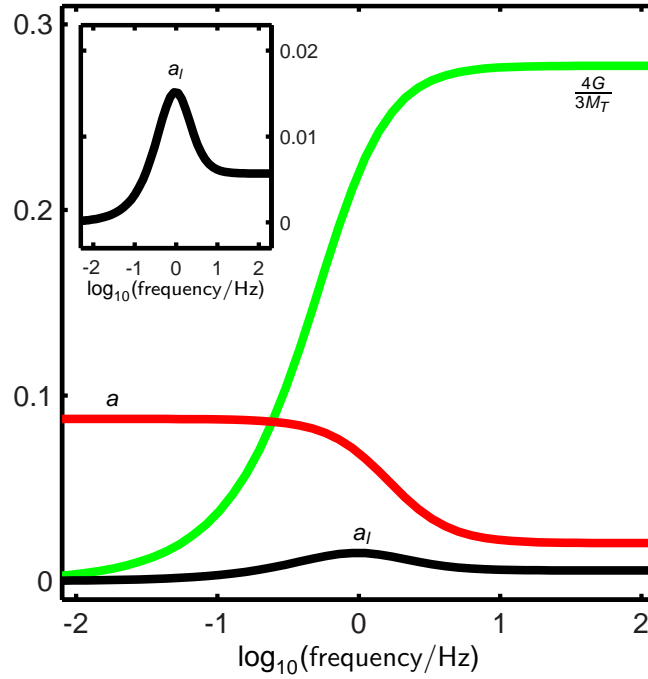


FIG. 1: Sketch of overlapping relaxations of $4G/(3M_T)$ (green) and the thermomechanical coupling, $a = T\alpha_p^2 K_T/c_p$ (red). The longitudinal coupling constant $a_l = (c_l - c_p)/c_p$ (black) is the product of those two frequency dependent functions. Near the crossing of the two curves the difference between c_l and c_p is generally largest. This determines the time scale of experiments on glass-forming liquids, where the cooling-by-heating effect is particularly large.

heat, c_V and the isochoric pressure coefficient β_V :

$$\sigma_{ij} + p\delta_{ij} = 2G(\epsilon_{ij} - \frac{1}{3}\epsilon\delta_{ij}) \quad (4)$$

$$p = -K_T\epsilon + \beta_V\delta T \quad (5)$$

$$\delta\mathcal{J} = \beta_V\epsilon + \frac{c_V}{T_0}\delta T. \quad (6)$$

We follow Biot [7] in assigning the symbol β to the thermodynamic pressure coefficient

$$\beta_V = \left(\frac{\partial p}{\partial T}\right)_V = \left(\frac{\partial S}{\partial V}\right)_T = \alpha_p K_T. \quad (7)$$

The material is furthermore characterized by the heat conductivity, λ , which enters Fourier's law for the entropy current density \mathbf{j}_s :

$$\mathbf{j}_s = -\frac{\lambda}{T_0}\nabla T. \quad (8)$$

The interest in thermoelastic problems has since Duhamel [8] mostly been focused on the calculation of thermal stresses deriving from an evolving temperature field. In the classical thermoelasticity theory the displacement field and temperature fields are partially decoupled [9, 10]. This comes from assuming that the development of the temperature can be found independently of the stresses by the conventional heat-diffusion equation:

$$\frac{\partial\delta T}{\partial t} = D\nabla^2\delta T. \quad (9)$$

Here D is a heat diffusion constant. After solving this equation the displacement field can be found from the quasi-static stress equilibrium equation:

$$M_T\nabla(\nabla\cdot\mathbf{u}) - G\nabla\times(\nabla\times\mathbf{u}) - \beta_V\nabla\delta T = \mathbf{0} \quad (10)$$

This approximate theory is referred to as the theory of thermal stresses [9]. According to many authors [9, 11–13] the correct treatment appeared remarkably late in the development of thermoelastic theory with Biot's paper [7] in 1956. Lessen [14] considered similar problems the same year. The heat diffusion equation Eq. (9) is replaced by

$$c_V \frac{\partial \delta T}{\partial t} + T_0 \beta_V \frac{\partial \nabla \cdot \mathbf{u}}{\partial t} = \lambda \nabla^2 \delta T, \quad (11)$$

which follows from entropy conservation

$$\frac{\partial \mathcal{J}}{\partial t} = -\nabla \cdot \mathbf{j}_\mathcal{J} \quad (12)$$

when this is combined with Eqs. (6) and (8). Entropy conservation may seem strange at first sight, but the entropy production per volume associated with heat conduction is $-\mathbf{j}_\mathcal{J} \cdot \frac{1}{T_0} \nabla T = \frac{\lambda}{T_0^2} (\nabla T)^2$, i.e., a second-order effect disappearing in a linearized theory.

In most cases the ordinary, decoupled heat-diffusion equation is a good approximation in the manner it is used in the theory of thermal stresses. However, this approximate theory is not able to describe the phenomenon of cooling by heating, which is the theme of this paper. It should be noted that the heat-diffusion equation with the diffusion constant containing the isobaric specific heat c_p is exact for the non-viscous liquid state or soft matter with $G = 0$, if part of the boundary (with normal vector \mathbf{n}) is free to expand, i.e., $\sum_j \sigma_{ij} n_j = 0$. The proof runs as follows: The assumption $G/M_T = 0$ simplifies Eq. (10) to

$$\nabla (K_T \nabla \cdot \mathbf{u} - \beta_V \delta T) = \mathbf{0}. \quad (13)$$

However, the terms under the gradient is according to Eq. (5) nothing but minus the pressure increment. Thus we conclude this pressure increment is uniform in space and only depends on time. Moreover, Eq. (4) ensures that all diagonal elements of the stress tensor are identical and equal to minus this pressure increment. If the normal component $\sum_j \sigma_{ij} n_j$ is zero on part of the boundary, it follows that the pressure is also zero there, but then it is zero throughout the body. Equation (5) then reduces to $\nabla \cdot \mathbf{u} = \alpha_p \delta T$. Inserting this in the entropy equation Eq. (11), one arrives at the ordinary decoupled heat diffusion equation with $D_p = \lambda/c_p$

$$\frac{\partial \delta T}{\partial t} = D_p \nabla^2 \delta T, \quad (14)$$

when noticing that $c_p = c_V + T_0 \frac{\beta_V^2}{K_T} = c_V + T_0 \alpha_p^2 K_T$.

As we have seen, the temperature field in general does not exactly obey a diffusion equation. It does so when $c_p = c_V$ ($\Leftrightarrow \beta_V = 0$) or for certain boundary conditions when $G = 0$. However, as emphasized by Biot [7], the entropy density in fact does fulfill a diffusion equation and moreover with a diffusion constant containing the ubiquitous longitudinal specific heat: Applying the divergence operator to the inertia-free stress equilibrium equation Eq. (10), gives

$$\nabla^2 \epsilon = \frac{\beta_V}{M_T} \nabla^2 \delta T. \quad (15)$$

Applying the Laplacian to the constitutive equation (6) yields

$$\nabla^2 \mathcal{J} = \left(\frac{\beta_V^2}{M_T} + \frac{c_V}{T_0} \right) \nabla^2 \delta T. \quad (16)$$

Fouriers law and the entropy conservation Eq. (12) gives

$$\frac{\partial \mathcal{J}}{\partial t} = \frac{\lambda}{T_0} \nabla^2 \delta T, \quad (17)$$

and thus

$$\frac{\partial \mathcal{J}}{\partial t} = \frac{\lambda}{c_l} \nabla^2 \mathcal{J}, \quad (18)$$

with $c_l = c_V + T_0 \frac{\beta_V^2}{M_T}$ being the longitudinal specific heat [1, 2].

Note that this result is limited to the inertia-free cases. If one wishes to study coupled mechanical and thermal waves, the inertia-term $\rho \frac{\partial^2}{\partial t^2} \mathbf{u}$ must be added on the right side of Eq. (10). Solutions of the equations in this case have been studied extensively [9] also in the spherically symmetric situation. Note, however, that acoustic wavelengths are much longer than

thermal wavelengths. Thus for a sample of a certain size there is an interesting time regime where acoustic waves have settled, but thermal diffusion has barely begun. Take as an example a sphere of radius 1cm. For a typical sound velocity of 10^3 m/s and heat diffusion constant of 10^{-7} m²/s, the sound traveling time is $10 \mu\text{s}$ while the diffusion time is 1 ks. It is within this time regime we will find the cooling-by-heating phenomenon. Although the solution restricted to the inertia-free case that we present below is in principle contained in the coupled acoustic-thermal wave solutions including inertia, the phenomenon is obscured by the complicated structure of these solutions and seems not to have been recognized.

The thermoelastic theory that was originally developed for elastic solids without relaxation is easily extended to a thermoviscoelastic theory taking relaxation of all the constitutive parameters into account, as it is necessary for relaxing liquids near the glass transition. The most straightforward way of generalizing is to interpret the equations in the frequency domain allowing all the constitutive parameters to be complex functions of the angular frequency ω . The cases we study in the frequency domain cover thus both solids and thermoviscoelastic liquids, but can only be transformed analytically into the time domain for solids. For relaxing liquids one must do the transformation numerically.

III. ANALYTICAL SOLUTIONS OF THE SPHERE-HEATING PROBLEM

A. The case when the heat flow is controlled at a mechanically free boundary

This subsection presents the analytical solution in the frequency domain to the situation when a sphere of a general viscoelastic material is subjected to a periodic heat input at the surface. The solution shows the temperature in the center at high frequencies varying 180° out-of-phase with respect to the heat oscillation at the surface, indicating the cooling-by-heating effect. In order to give a more lucid and transparent understanding of the phenomenon we translate the solution to the time domain. This can be done analytically by an inverse Laplace transformation if there is no frequency dependence of the constitutive properties. That is, we calculate the temperature and stress profile throughout the sphere following a heat-step input at the surface at time zero.

Consider the case when a periodically varying heat $\delta Q(t) = \text{Re} \{ \delta Q e^{i\omega t} \}$ is supplied at the surface of a sphere of radius R . The surface is assumed to be mechanically non-clamped, i.e., the sphere is free to expand. This translates into the boundary condition that the radial component of the stress tensor is zero at the surface, $\sigma_{rr}(R, \omega) = 0$. We wish to calculate how the periodically varying temperature and displacement fields vary throughout the sphere, i.e., to calculate the complex frequency-dependent amplitudes of temperature, $\delta T(r, \omega)$, and radial displacement field, $u(r, \omega)$. From these quantities the stress components $\sigma_{rr}(r, \omega)$, etc, may be calculated.

Denoting the angular frequency by ω , the position vector by \mathbf{r} , the complex frequency-dependent radial displacement field by $\mathbf{u}(r, \omega) = u(r, \omega)\mathbf{r}/r$, the coupled thermoelastic equations (10) and (11) become

$$\frac{\partial}{\partial r} \left[M_T r^{-2} \frac{\partial}{\partial r} (r^2 u) - \beta_V \delta T \right] = 0 \quad (19)$$

$$(i\omega)c_V \delta T + (i\omega)T_0 \beta_V r^{-2} \frac{\partial}{\partial r} (r^2 u) = \lambda r^{-2} \frac{\partial}{\partial r} (r^2 \frac{\partial}{\partial r} \delta T). \quad (20)$$

The four boundary conditions are:

1. No displacement at the center: $u(0, \omega) = 0$;
2. No temperature gradient at the center: $\frac{\partial \delta T}{\partial r}(0, \omega) = 0$;
3. Free surface, i.e., no radial stresses at the surface: $\sigma_{rr}(R, \omega) = 0$;
4. Heat supply boundary condition at the surface: $\lambda \frac{\partial \delta T}{\partial r}(R, \omega) = i\omega \frac{\delta Q}{4\pi R^2}$.

Denote the volume of the sphere by $V_0 = \frac{4}{3}\pi R^3$ and define the complex frequency-dependent thermal wavevector by $k = \sqrt{i\omega c_l(\omega)/\lambda}$. Define furthermore the functions

$$f_1(r/R, k^2 R^2) = \frac{1}{3} \frac{\sinh(kr)}{kr} \frac{(kR)^3}{kR \cosh(kR) - \sinh(kR)} \quad (21)$$

$$f_2(r/R, k^2 R^2) = \left(\frac{R}{r}\right)^3 \frac{(kr) \cosh(kr) - \sinh(kr)}{(kR) \cosh(kR) - \sinh(kR)}. \quad (22)$$

Introduce the characteristic heat diffusion time

$$\tau = (c_l(\omega)/\lambda)R^2. \quad (23)$$

Then one has $k^2 R^2 = i\omega\tau$ and the solutions to Eqs. (19) and (20) are

$$\delta T(r, \omega) = \frac{1}{V_0 c_l} \{-a_l + f_1(r/R, i\omega\tau)\} \delta Q \quad (24)$$

$$u(r, \omega) = \frac{1}{3} \frac{\alpha_p}{V_0 c_p} r \left\{ \frac{4}{3} \frac{G}{M_S} + \frac{K_S}{M_S} f_2(r/R, i\omega\tau) \right\} \delta Q. \quad (25)$$

These solutions were found by the transfer-matrix approach (see Ref. 2 and Appendix A 1), and can be verified by insertion, noticing that $f_1(\rho, s) = \frac{1}{3\rho^2} \frac{\partial}{\partial \rho} (\rho^3 f_2(\rho, s))$, $\frac{\partial}{\partial \rho} f_1(\rho, s) = \frac{1}{3} \rho s f_2(\rho, s)$ and $\frac{1}{\rho^2} \frac{\partial}{\partial \rho} \rho^2 \frac{\partial}{\partial \rho} f_1(\rho, s) = s f_1(\rho, s)$.

Consider the low- and high-frequency limits of these expressions. The functions f_1 and f_2 both have the limits 1 for $\omega \rightarrow 0$ and 0 for $\omega \rightarrow \infty$. Thus, as expected $\delta T \rightarrow \delta Q / (V_0 c_p)$ in the low-frequency limit when heat has had time to distribute throughout the sphere. At high frequency the temperature amplitude becomes

$$\delta T(r) \rightarrow -\frac{1}{V_0 c_l} a_l \delta Q = -\frac{1}{V_0} \left(\frac{1}{c_l} - \frac{1}{c_p} \right) \delta Q \quad \text{for } \omega \rightarrow \infty. \quad (26)$$

If we for a moment consider the non-relaxing case where the specific heats are real, we see that the temperature amplitude is in counter-phase to the heat amplitude since $c_l < c_p$. For a propagating thermal wave it would not be surprising that temperatures at some distance – e.g., at a half wavelength – had opposite phases. However, Eq. (26) holds throughout the sphere and is not associated with the diffusive thermal wave. This will be even more clear when we consider the response to a heat step input later on.

We see that the longitudinal coupling constant a_l controls the magnitude of the cooling-by-heating effect. The ratio of the amplitudes of the temperature in the center and the heat input at the surface is shown in Fig. 2. The phenomenon “cooling by heating” is indicated at high frequencies, albeit this is more conspicuous in the time domain.

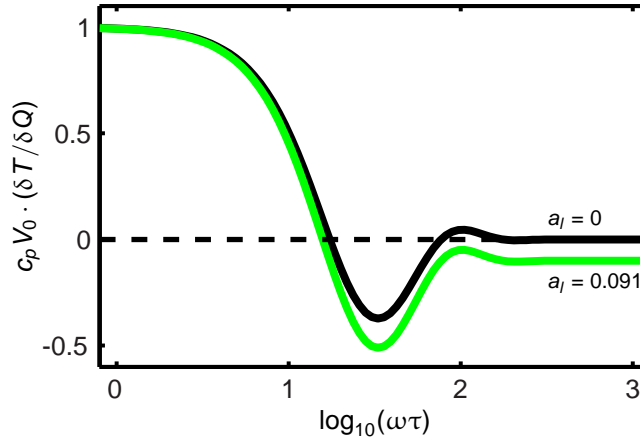


FIG. 2: The real part of the ratio between the complex amplitudes of temperature at the center and the heat supplied at the surface scaled with the isobaric heat capacity. At high frequencies the limit becomes the negative value $-a_l / (1 - a_l) = 1 - c_p / c_l$.

For the displacement field we find for the low-frequency limit the natural result,

$$u(r) \rightarrow \frac{1}{3} \alpha_p \frac{\delta Q}{V_0 c_p} r \quad \text{for } \omega \rightarrow 0 \quad (27)$$

determined by the final temperature rise $\frac{\delta Q}{V_0 c_p}$ and the linear thermal expansion $\frac{1}{3} \alpha_p$. However, at high frequencies we find

$$u(r) \rightarrow \frac{1}{3} \alpha_p \frac{\delta Q}{V_0 c_p} \frac{4G}{3M_S} r \quad \text{for } \omega \rightarrow \infty. \quad (28)$$

Notice that this displacement, which is responsible for the cooling-by-heating effect, is only present when $G \neq 0$.

In the spherically symmetric case there are only two different components of the stress tensor, σ_{rr} and $\sigma_{\theta\theta} = \sigma_{\phi\phi}$. It follows from Eqs. (4) and (5) and the fact that $\epsilon_{rr} = \frac{\partial u}{\partial r}$ and $\epsilon_{\theta\theta} = \epsilon_{\phi\phi} = \frac{u}{r}$ that $\sigma_{rr} = (K_T + \frac{4}{3}G) \frac{\partial u}{\partial r} + 2(K_T - \frac{2}{3}G) \frac{u}{r} - \beta_V \delta T$, which by Eqs. (24) and (25) becomes

$$\sigma_{rr}(r, \omega) = \frac{4}{3} \frac{G}{M_T} \frac{\beta_V}{V_0 c_l} \{1 - f_2(r/R, i\omega\tau)\} \delta Q. \quad (29)$$

Likewise, $\sigma_{\theta\theta} = (K_T - \frac{2}{3}G)\frac{\partial u}{\partial r} + 2(K_T + \frac{1}{3}G)\frac{u}{r} - \beta_V\delta T$, which becomes

$$\sigma_{\theta\theta}(r, \omega) = \frac{4}{3} \frac{G}{M_T} \frac{\beta_V}{V_0 c_l} \left\{ 1 - \frac{3}{2} f_1(r/R, i\omega\tau) + \frac{1}{2} f_2(r/R, i\omega\tau) \right\} \delta Q. \quad (30)$$

Thus at high frequencies there is an isotropic, uniform tensile stress in the interior of the sphere of the magnitude

$$\sigma_{rr}, \sigma_{\theta\theta}, \sigma_{\phi\phi} \rightarrow \frac{4}{3} \frac{G}{M_T} \frac{\beta_V}{V_0 c_l} \delta Q \quad \text{for } \omega \rightarrow \infty \quad (31)$$

On the other hand, all stresses vanish for $\omega \rightarrow 0$ (as expected).

In order to gain insight into the cooling-by-heating effect and show the significance of the longitudinal coupling constant a_l we transform Eqs. (24), (29) and (30) into the time domain, but only for a solid, i.e., in the case when all constitutive properties are frequency independent. If a delta function heat flux is applied at $t = 0$, the heat supplied at the surface is a Heaviside step function, $\delta Q(R, t) = \delta Q_0 H(t)$; in this case calculating the inverse Laplace-Stieltjes transform leads to the following expressions for the temperature and stresses as functions of time after $t = 0$ (see Appendix A 2):

$$\delta T(r, t) = \frac{1}{c_l V_0} \{-a_l + F_1(r/R, t/\tau)\} \delta Q_0, \quad (32)$$

$$\sigma_{rr}(r, t) = \frac{4}{3} \frac{G}{M_T} \frac{\beta_V}{V_0 c_l} \{1 - F_2(r/R, t/\tau)\} \delta Q_0, \quad (33)$$

$$\sigma_{\theta\theta}(r, t) = \frac{4}{3} \frac{G}{M_T} \frac{\beta_V}{V_0 c_l} \left\{ 1 - \frac{3}{2} F_1(r/R, t/\tau) + \frac{1}{2} F_2(r/R, t/\tau) \right\} \delta Q_0, \quad (34)$$

where

$$F_1(r/R, t/\tau) = 1 + \frac{2}{3} \frac{R}{r} \sum_{n=1}^{\infty} \frac{\sin(\frac{r}{R} x_n)}{\sin(x_n)} e^{-x_n^2 t/\tau} \quad (35)$$

$$F_2(r/R, t/\tau) = 1 + 2 \left(\frac{R}{r}\right)^3 \sum_{n=1}^{\infty} \frac{\sin(\frac{r}{R} x_n) - \frac{r}{R} x_n \cos(\frac{r}{R} x_n)}{x_n^2 \sin(x_n)} e^{-x_n^2 t/\tau}. \quad (36)$$

Here $x_1 < x_2 < \dots$ are the positive roots of the transcendental equation $x = \tan(x)$. Note that F_1 and $F_2 \rightarrow 0$ for $t \rightarrow 0$ and F_1 and $F_2 \rightarrow 1$ for $t \rightarrow \infty$. When $a_l = 0$ there is no cooling-by-heating effect according to Eq. (32). Furthermore, $a_l = 0$ implies either $G = 0$ or $\beta_V = 0$ and there is no immediate expansion and no induced stresses.

When $a_l \neq 0$ the situation is quite different. In Fig. 3 we plot the scaled temperature change $(c_p V_0 / \delta Q) \delta T(t/\tau; r/R)$ for a several radii r/R as given in Eq. (32). The longitudinal coupling constant is here fixed to $a_l = 0.091$ and time is given in units of the characteristic heat diffusion time τ . The figure clearly shows the cooling-by-heating effect. Since a finite amount of heat was added at the surface at $t = 0$, the surface temperature initially diverges. The interior of the sphere, even close to the surface, instantaneously cools to a uniform temperature. The expansion of the surface is immediately felt in the interior, and since no heat has yet arrived by diffusion, it cools adiabatically. This initial response is followed by an evolution in time where the temperatures of the different parts of the sphere converge and eventually equilibrate.

In order to understand better the physics of cooling-by-heating we consider the components of the stresses given by Eqs. (33) and (34), respectively. In Fig. 4 the σ_{rr} component of the stress tensor is plotted scaled with the initial uniform interior stress $\sigma_0 = \frac{4}{3} \frac{G}{M_T} \frac{\beta_V}{V_0 c_l} \delta Q_0$. First we note that the boundary condition $\sigma_{rr}(R, t) = 0$ is fulfilled. As the surface receives heat and expands, an immediate traction is felt in the interior of the sphere. σ_{rr} is positive, seeking to stretch a volume element in the radial direction under the entire evolution to thermal equilibrium.

The scaled stress component $\sigma_{\theta\theta}(r, t)$, is shown in Fig. 5. One notices an immediate, uniform increase of this stress component throughout the sphere of the same size as σ_{rr} . The initial stress is thus isotropic. Note that $\sigma_{\theta\theta}$ shifts sign during the thermal equilibration process, in contrast to σ_{rr} . This can be understood in a physical picture: Consider the outer region that has been reached by the inflowing heat at a certain point in time. If that region were free it would expand, but it is kept in place by the inner unheated region that has not expanded thermally yet. This creates a negative stress on surfaces with normal at right angle to the radius vector.

We conclude this section by a simple result. If one compares the instantaneous temperature drop Eq. (26) and the instantaneous stress increase Eq. (31), one finds that the ratio is given by the adiabatic temperature—pressure coefficient:

$$\frac{\delta T(r < R, t = 0)}{\delta p(r < R, t = 0)} = 1/\beta_S = \left(\frac{\partial T}{\partial p}\right)_S. \quad (37)$$

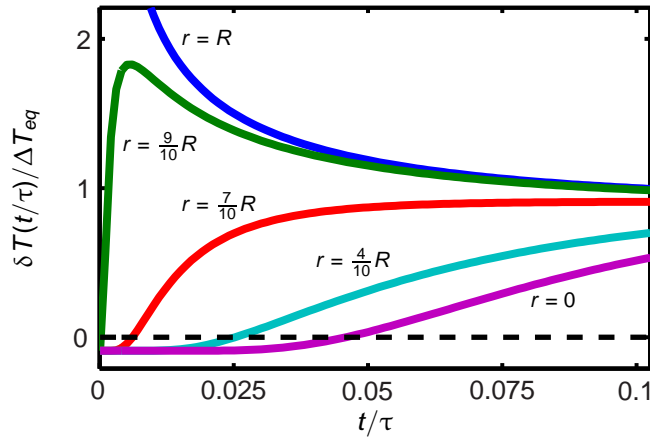


FIG. 3: The temperature of the sphere as a function of time for different radii normalized to the final temperature $\Delta T_{eq} = \delta Q_0 / (V_0 c_p)$. After addition of heat at the surface, the temperature drops instantaneously throughout the sphere, showing adiabatic cooling. The time scale is given by the characteristic heat diffusion time, $\tau = R^2 c_l / \lambda$. The longitudinal coupling constant is chosen to $a_l = 0.091$.

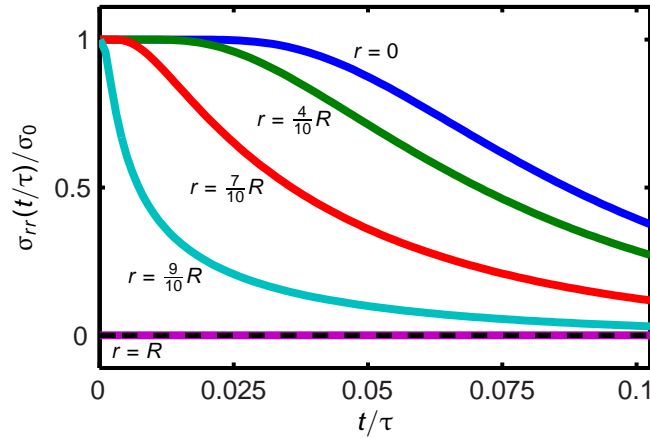


FIG. 4: The rr -component of the stress tensor, $1 - F_2$, as a function of time for a number of radii scaled with the initial stress, $\sigma_0 = \frac{4}{3} \frac{G}{M_T} \frac{\beta_V}{V_0 c_l} \delta Q_0$. After the addition of heat at the surface, σ_{rr} immediately increases throughout the sphere. The stress is released as heat diffuses towards the center from the surface.

B. The case when temperature is controlled at a mechanically free boundary

The above studied case with heat-input control showed a rather simple cooling-by-heating behavior at short times or high frequencies. We now consider the case of controlling the temperature on the outer surface instead. There is still an effect, but it is not instantaneous. We only calculate the temperature in the center of the sphere. The surface is again mechanically free. Again, using the transfer matrix technique in the frequency domain, one finds that the temperature amplitude, $\delta T(0, s)$ in the center is related to the temperature amplitude, $\delta T(R, s)$ at the surface by $\delta T(0, s) = \Phi(s) \delta T(R, s)$, where

$$\Phi(s) = \left(1 - \frac{x^3 - x^2 \sinh(x)}{3a_l [x \cosh(x) - \sinh(x)] - x^2 \sinh(x)} \right). \quad (38)$$

Here $x = \sqrt{s\tau(\omega)}$, $s = i\omega$. The characteristic diffusion time $\tau(\omega)$ (Eq. (23)) and thermomechanical coupling constant $a_l(\omega)$ (Eq. (2)) are in the general thermoviscoelastic case complex and frequency dependent and the temperature response can only be converted to the time domain numerically.

In order to calculate the temperature signal as a function of time we again limit ourselves to the purely thermoelastic case, i.e., the case of a solid where τ and a_l are real and frequency independent. For a Heaviside temperature step at the surface of the sphere, $\delta T(R, t) = \Delta T H(t)$, the temperature at the sphere center is calculated via an inverse Laplace-Stieltjes transform of

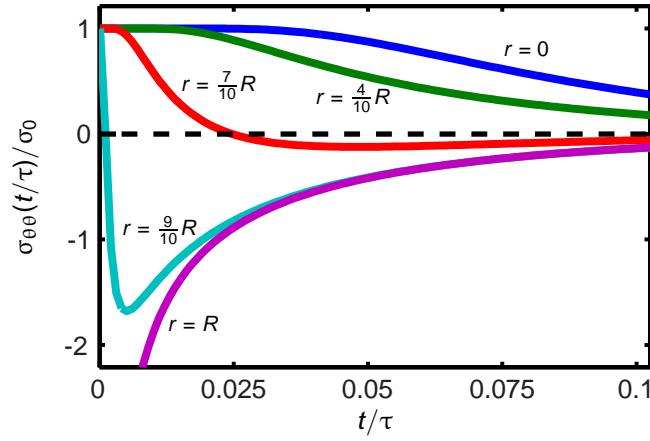


FIG. 5: The $\theta\theta$ -component of the stress tensor, $1 - \frac{3}{2}F_2 + \frac{1}{2}F_1$, as a function of time scaled with the initial stress σ_0 . There is an initial adiabatic positive step up in $\sigma_{\theta\theta}$ throughout the sphere. The regions that have been reached by the incoming diffusive heat at a certain point in time experience a negative $\theta\theta$ -stress component since the inner unheated regions pull the outer heated regions inwards.

$\Phi(s)$,

$$\delta T(0, t) = \Delta T \left\{ 1 - \sum_{k=0}^{\infty} R_k \exp\left(-y_k^2 \frac{t}{\tau}\right) \right\}, \quad (39)$$

where the residues are given by

$$R_k = \frac{2(1 - \cos y_k) + y_k \sin y_k / (3a_l)}{(1 - 3a_l) \cos y_k + y_k(2 - 3a_l) \sin y_k}. \quad (40)$$

Here the y_k 's denote the positive roots of the transcendental equation

$$\cot(y) = \frac{1}{y} - \frac{y}{3a_l}. \quad (41)$$

In Fig. 6 we plot the solution Eq. (39) for various values for the coupling constant a_l . Time is given in units of the characteristic diffusion time and $\Delta T = 1\text{K}$. We see that the cooling-by-heating effect is present also when a step in temperature (instead of heat) is applied to the surface. However, now the effect is not instantaneous but evolves gradually, reflecting the gradual heat diffusion at the surface mediated by the stress field. Figure (6) furthermore shows that it is not enough to have a thermomechanical coupling ($\alpha_p \neq 0$) for the phenomenon to be present – only when $c_l \neq c_p$ is there a cooling-by-heating effect. The next section studies the general, thermoviscoelastic case of frequency dependence of the response functions, which describes supercooled liquids.

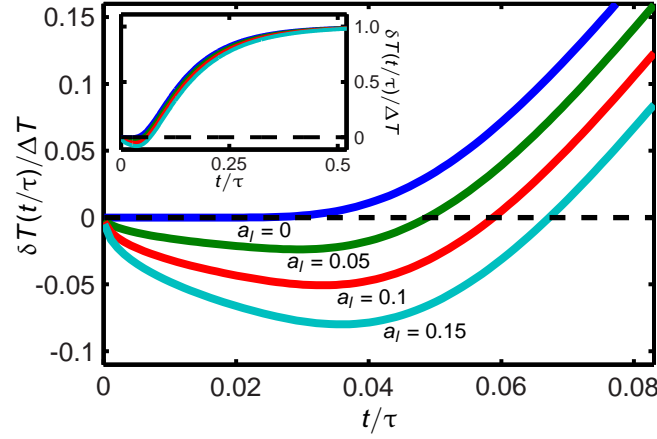


FIG. 6: The temperature at the center of the sphere as a function of time. After the temperature at the surface has been raised, the temperature at the center of the sphere initially decreases. This only happens when $c_l \neq c_p$, i.e., when the longitudinal coupling a_l is not negligible. The temperature step at the boundary is $\Delta T = 1\text{K}$, and the time scale is given by the characteristic diffusion time, $\tau = R^2 c_l / \lambda$.

IV. THE THERMOVISCOELASTIC CASE

The above time-domain results apply for a thermoelastic solid only, whereas the frequency-domain results are general. The thermoelastic examples handled so far only involved frequency-*independent* constitutive parameters, corresponding to the high-frequency (low-temperature) limiting values of the curves sketched in Fig. 1. However, Fig. 1 indicates that the value of the coupling constant a_l is larger at lower frequencies (higher temperature), thus suggesting that the effect of cooling by heating may be even larger in the very viscous liquid or simply at the glass transition. We investigate this issue in the time domain in this section. In the thermoelastic case the inversion of the problem to the time-domain could be made analytically. This is not possible in the thermoviscoelastic case where the constitutive parameters are complex frequency-dependent functions.

In order to investigate the effect of going from solid to liquid we resort to numerical methods. Specifically, we transform $\Phi(s)$ of Eq. (38) into the time-domain, accounting for the frequency-dependence of the constitutive parameters via τ and a_l . To do this we have to introduce a model of the constitutive parameters that enters via τ and a_l . It is common in rheology to illustrate models like the Maxwell model by rheological networks or even their electrical analogue. We use this approach to model the thermoviscoelastic behavior. The purpose of the model is to interpolate between the thermodynamic coefficients at high frequencies, $\kappa_{T,\infty}, c_{p,\infty}, \alpha_{p,\infty}$ and at low frequencies $\kappa_{T,0}, c_{p,0}, \alpha_{p,0}$. Network modeling assures internal consistency and agreement with the rules of linear irreversible thermodynamics. A one-parameter relaxation model implies the Prigogine-Defay ratio is unity, which is not the case for glucose. Rather, with $T_g = 300\text{K}$ and $\Delta c_p = 1.14 \cdot 10^6 \text{JK}^{-1}\text{m}^{-3}$, $\Delta \kappa_T = 6.1 \cdot 10^{-11} \text{Pa}^{-1}$ and $\Delta \alpha_p = 2.6 \cdot 10^{-4} \text{K}^{-1}$ one finds

$$\Pi = \frac{\Delta c_p \Delta \kappa_T}{T_g (\Delta \alpha_p)^2} = 3.4. \quad (42)$$

We are thus forced to consider a model with two relaxation elements that cannot be lumped into one. The model of Fig. 7 is suited for this purpose. In order to still make it simple, the two relaxing elements are taken to be Debye-like. The model has a simple mathematical formulation in the frequency domain. We change the independent variables compared to Eqs. (5) and (6) and consider the complex amplitude δT and δp to be the controlled stimuli creating a linear response in the amplitudes $\delta \mathcal{J}$ and $\delta \epsilon$ of the entropy density and dilation:

$$\begin{pmatrix} \delta \mathcal{J} \\ \delta \epsilon \end{pmatrix} = \begin{pmatrix} \zeta_p(\omega) & \alpha_p(\omega) \\ \alpha_p(\omega) & \kappa_T(\omega) \end{pmatrix} \cdot \begin{pmatrix} \delta T \\ -\delta p \end{pmatrix}. \quad (43)$$

Here $\zeta_p = c_p/T_0$, $\alpha_p = \beta_V/K_T$, $\zeta_p = \zeta_V + \beta_V^2/K_T$ and $\kappa_T = 1/K_T$. In the model the three measurable quantities, the isobaric specific heat, the isobaric expansivity, and the isothermal compressibility are related to the elements $D, C, J_A(\omega)$, and $J_B(\omega)$ by

$$\zeta_p = D^2 J_A(\omega) + C, \quad (44)$$

$$\alpha_p = -D J_A(\omega), \quad (45)$$

$$\kappa_T = J_A(\omega) + J_B(\omega). \quad (46)$$

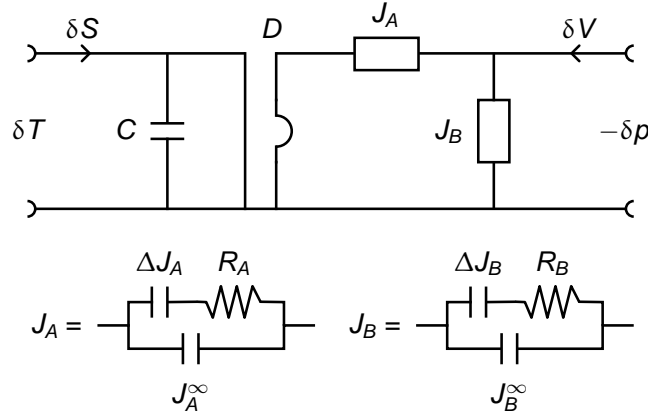


FIG. 7: Electrical equivalent diagram of the interaction of a volume element with its surroundings through two gates. The thermal gate where entropy displacement δS or temperature δT can be controlled, and the mechanical gate where volume displacement δV or pressure δp can be controlled. δS and δV are generalized charge displacements and δT and $-\delta p$ are generalized voltages. The relaxational elements J_A and J_B are simple single relaxation time elements.

The relaxing element J_A is determined by three parameters $J_{A,\infty}$, $\Delta J_A = J_{A,0} - J_{A,\infty}$ and R_A :

$$J_A = J_{A,\infty} + \frac{1}{\frac{1}{\Delta J_A} + i\omega R_A} \quad (47)$$

and likewise for J_B .

The parameters of the model can be established from the high and low frequency limits of ζ_p , κ_T and α_p . One finds $D = -\Delta\zeta_p/\Delta\alpha_p$, $J_{A,0} = -\alpha_{p,0}/D$, $J_{A,\infty} = -\alpha_{p,\infty}/D$, $J_{B,0} = \kappa_{T,0} - J_{A,0}$ and $J_{B,\infty} = \kappa_{T,\infty} - J_{A,\infty}$. The Prigogine-Defay ratio of the model is given by

$$\Pi = \frac{\Delta\zeta_p \Delta\kappa_T}{(\Delta\alpha_p)^2} = 1 + \frac{\Delta J_B}{\Delta J_A}, \quad (48)$$

and the dynamic (frequency-dependent) Prigogine-Defay ratio [15] is given by

$$\Lambda = \frac{\zeta_p'' \kappa_T''}{(\alpha_p'')^2} = 1 + \frac{J_B''}{J_A''} \quad (49)$$

As expected, the Prigogine-Defay ratio is larger than unity, but becomes one if the element J_B is non relaxing, in which case the model reduces to a single-parameter model. In the case of J_A being non-relaxing, the model degenerates with absence of relaxation in ζ_p and α_p . For glucose at 300K we calculate the parameters of the model to be $D = -1.46 \cdot 10^7 \text{ PaK}^{-1}$, $C = 4.76 \cdot 10^3 \text{ JK}^{-1}\text{m}^{-3}$, $J_{A,\infty} = 7.53 \cdot 10^{-12} \text{ Pa}^{-1}$, $\Delta J_A = 1.78 \cdot 10^{-11} \text{ Pa}^{-1}$, $J_{B,\infty} = 8.55 \cdot 10^{-11} \text{ Pa}^{-1}$, and $\Delta J_B = 4.33 \cdot 10^{-11} \text{ Pa}^{-1}$.

The heat conductivity of glucose — needed to calculate the heat diffusion time — is $\lambda = 0.35 \text{ WK}^{-1}\text{m}^{-1}$ at 303 K according to Greene and Parks [16]. The shear relaxation of glucose is modeled by a Maxwell model

$$G(\omega) = \frac{1}{\frac{1}{G_\infty} + \frac{1}{i\omega\eta}}. \quad (50)$$

Here the high-frequency shear modulus can be taken to be $G_\infty = 3.1 \cdot 10^9 \text{ Pa}$ [5]. The values of the thermodynamic parameters used to parametrize the model are given in Table I. The temperature dependence of the shear viscosity causes the shift in the loss peaks of the relaxations. Parks *et al.* [17] measured the viscosity of glucose in a wide temperature range from 295K to 418K. We fitted their tabulated data by the expression $\eta(T) = 0.0125 \exp((512.9\text{K}/T)^{6.42}) \text{ Pas}$. This holds within 20% over the entire temperature range except for the highest viscosity point of $9.1 \cdot 10^{12} \text{ Pas}$, which however is well beyond the glass transition and may be hard to measure reliably. A Vogel-Fulcher law is not as good a fit, deviating more than 40% in the measured temperature range. The rate parameters $R_A = R_A(T)$ and $R_B = R_B(T)$ are assumed to follow the temperature dependence of the viscosity [18]. It is found numerically that one should chose $R_A(T) = R_B(T) = 30\eta(T)$ in order to get the loss-peak frequency of the shear modulus, $G(\omega)$, and isothermal bulk modulus, $K_T(\omega)$, to coincide. The relaxation of the different response functions

Quantity	Value	Reference
$\omega \rightarrow 0$		
$\kappa_{T,0}$	$15.4 \cdot 10^{-11} \text{Pa}^{-1}$	[4]
$c_{p,0}$	$3.05 \cdot 10^6 \text{JK}^{-1}\text{m}^{-3}$	[3]
$\alpha_{p,0}$	$3.7 \cdot 10^{-4} \text{K}^{-1}$	[3]
λ (at 303K)	$0.35 \text{WK}^{-1}\text{m}^{-1}$	[16]
$\omega \rightarrow \infty$		
$\kappa_{T,\infty}$	$9.30 \cdot 10^{-11} \text{Pa}^{-1}$	[4]
$c_{p,\infty}$	$15.4 \cdot 10^{-11} \text{JK}^{-1}\text{m}^{-3}$	[3]
$\alpha_{p,\infty}$	$1.1 \cdot 10^{-4} \text{K}^{-1}$	[3]
G_∞	$3.1 \cdot 10^9 \text{Pa}$	[5]

TABLE I: Literature data for glucose (at 300K) used to parametrize the model depicted in the electrical equivalent diagram in Fig. 7. We have used a density of $1.52 \cdot 10^3 \text{kg m}^{-3}$ to convert specific heat data from mass to volume.

described by the model implies a frequency dependence of the longitudinal thermomechanical coupling via

$$a_l(\omega) = \frac{\frac{4}{3}G(\omega)T_0\alpha_p^2(\omega)}{(1 + \frac{4}{3}G(\omega)\kappa_T(\omega))c_p(\omega)}. \quad (51)$$

The modulus of this complex function was shown in Figure (1). Also, the heat-diffusion time

$$\tau(\omega) = R^2(1 - a_l(\omega))c_p(\omega)/\lambda \quad (52)$$

now becomes complex. This makes the inversion to the time-domain non-trivial and thus Eq. (38) was inverted numerically. The algorithm for the inverse Laplace transform is an improved version of de Hoog's quotient difference method [19] developed and implemented in Matlab by Hollenbeck [20].

The calculated temperature response in the middle of the sphere to a step of 1 K at the surface is shown in Fig. 8. Time is now scaled by the fixed real-valued diffusion time τ_0 in the liquid regime,

$$\tau_0 = R^2c_{p,0}/\lambda. \quad (53)$$

The figure shows that the effect of the thermomechanical coupling is absent at high temperatures. But as temperature is decreased and the liquid gets more and more viscous, a dip in temperature emerges. Going further down in temperature the phenomenon of cooling by heating becomes most pronounced slightly above T_g . Even further down in temperature, in the glassy state, the effect is still present, but small. One may ask what happens if the expansivity $\alpha_{p,\infty}$ vanishes, so that the phenomenon is absent in the glassy state: Will it still be present at the glass transition? The simulations shown in Fig. (9) confirm this expectation. Putting $\alpha_{p,\infty} = 0$, but otherwise keeping the values of the rest of the parameters, we get a succession of temperature evolutions. Going down in temperature we see the cooling-by-heating phenomenon appearing at T_g and afterward disappearing in the glassy state. Fig. 10 shows the minimum temperature δT_{MIN} reached when $\alpha_{p,\infty} \neq 0$ as a function of temperature T_0 , emphasizing the phenomenon as characteristic of the glass transition.

V. EXPERIMENTAL VERIFICATION OF THE COOLING-BY-HEATING EFFECT

To prove the existence of cooling by heating we molded glucose (α -D(+) glucose, 98%, Sigma-Aldrich) into spherical samples with a thermistor placed in the center. Via the large negative temperature coefficient (NTC) thermistor we measured the temperature in the middle of the sphere. During measurements the glucose sphere is placed in a cryostat, that makes it possible to change the temperature at the surface of the sphere quickly compared to the characteristic heat diffusion time. A sketch of the setup together with a photo of one of the samples is shown in Fig. 11. The photo shows the wires that lead into the sphere, connecting the thermistor to the terminals on the peek plate shown in the photo. When mounted on a holder, the terminals get connected to the multimeter that does the resistance measurement.

The procedure in the experiments was the following. First we brought down the temperature to the desired starting level. Then we waited for the temperature to equilibrate. This was monitored by measuring the resistance every fifth minute. Typical waiting time was 18 hours. After the initial waiting time, we increased the sampling rate of the multimeter to about five data points per minute. This was done for one hour to get a baseline like the one in Fig. 12. Then we imposed a 5K temperature step and

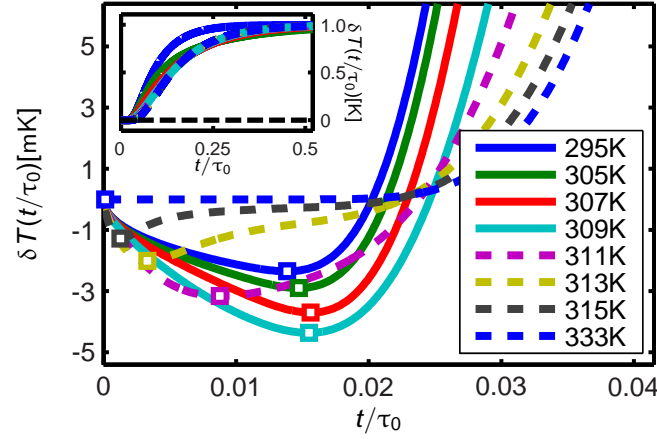


FIG. 8: The change in temperature, δT , at the center of a sphere, after a temperature step of $\Delta T = 1K$ has been applied at the surface. A model of the thermoviscoelastic relaxation of glucose with realistic limiting thermodynamic parameters has been invoked. Time is scaled by the characteristic diffusion time τ_0 , which is 800 s for a glucose ball of radius 9.5 mm. The minimum of approximately $-5mK$ occurs for the 309K curve just above T_g at $0.017\tau_0$, corresponding to 14 s. Notice that although the cooling-by-heating phenomenon is present in the glassy solid state, it becomes more pronounced at the glass transition. The squares marking the minima at each temperature are plotted against temperature in Fig. 10.

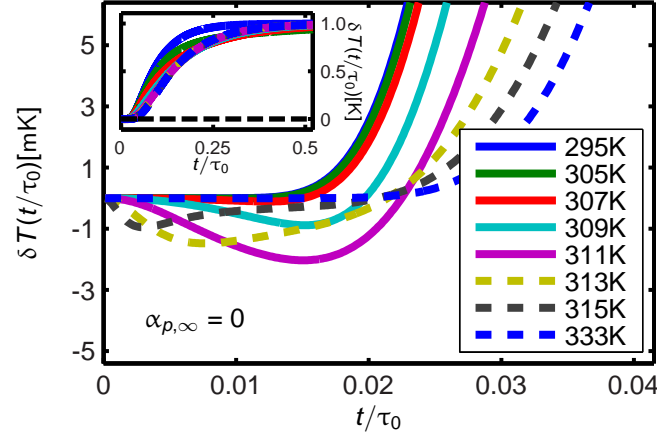


FIG. 9: A simulation similar to the one shown in Fig. (8) except that $\alpha_{p,\infty}$ has been put to 0, forcing cooling by heating to be absent in the glassy solid phase. It is seen that the cooling by heating effect still appears as a dynamic phenomenon at the glass transition.

continued sampling data for another ten minutes with a sampling rate of 15 data points per minute. Fig. 12 shows the temperature measured by the NTC thermistor during a measurement with a step from 298K to 303K of the cryostat temperature. The baseline extends for about 20 minutes, then a characteristic temperature dip appears. The magnitude of the dip is $7.3 \pm 0.2mK$, which was reached 40 seconds after the temperature step was imposed.

The experiment was repeated on three different samples; the inset in Fig. 12 shows the results of the first measurement done on each sample, at the same temperature. Each marker represents the lowest temperature reached in one measurement. They are plotted against time after the temperature step is initiated. It was not possible to reproduce the phenomenon on the same sample by recycling the temperature. We ascribe this to crystallization. Although the effect should be present also in the solid state, it is here considerably smaller and not observable with our temperature resolution. Nevertheless, the phenomenon was seen every time we repeated the experiment with a fresh supercooled sample. The sphere does not flow or deform to any appreciable degree even somewhat above the glass transition. The characteristic flow time τ_{flow} is proportional to the viscosity and inversely proportional to the gravitational force mg . By a dimensional argument it follows that

$$\tau_{flow} \propto \frac{\eta}{\rho g r} = \frac{G_{\infty}}{\rho g r} \tau_M, \quad (54)$$

which means that $\tau_{flow} \sim 10^7 \tau_M$. Thus even at 310 K, where viscosity becomes 10^{10} Pas and thereby the Maxwell time 3 s, the flow time is one year.

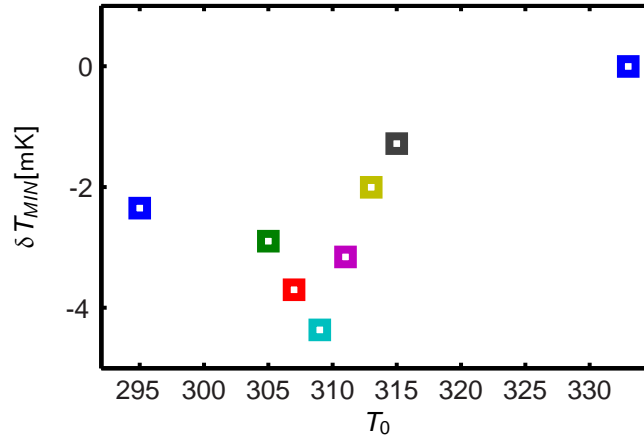


FIG. 10: The minima from Fig. 8 as a function of temperature. At high temperatures the phenomenon of cooling-by-heating is absent. Going down in temperature the liquid becomes more viscous and a dip in temperature emerges. Close to the glass transition the cooling-by-heating phenomenon gets most pronounced. As temperature is decreased further and the liquid enters the glassy state the effect is still present, however reduced in strength.

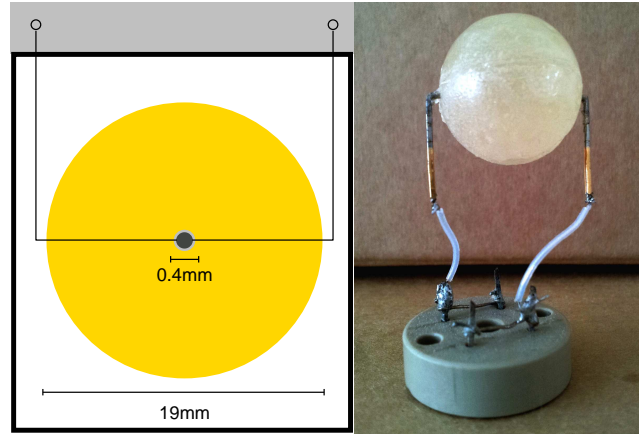


FIG. 11: Sketch of the experimental setup. The liquid is molded into a sphere, in which a small NTC-thermistor bead is placed in the center, connected to wires that lead to a multimeter that performs resistance measurements. The sphere is inserted into the cylindrical chamber of a cryostat. The photo shows one of the samples; at the time of the photo shoot (1 month after molding) the sample is no longer transparent because it crystallized.

VI. DISCUSSION

The concept of a longitudinal specific heat was identified in Ref. 1 as the relevant quantity within AC-calorimetric methods that utilize heat effusion. The principle of the simplest of these techniques [21] is to measure the complex temperature response T_ω at a plane surface to a heat current density $j_{Q,\omega}$ generated at the same surface. The effusivity $e = \sqrt{\lambda c}$ is found from the measured specific thermal impedance $Z \equiv T_\omega / j_{Q,\omega} = 1 / \sqrt{i\omega\lambda c}$, and from the effusivity the specific heat can be calculated. A meticulous analysis of the thermoelastic equations of this problem showed that the specific heat that comes into play in this situation is c_l rather than c_p . Effusivity measurements in spherical geometry have been shown also to involve the longitudinal specific heat [2, 22]. It is not a very well-known property, but it does appear in the textbook on elasticity by Landau and Lifshitz [23]. They show that the coupled thermoelastic equations decouple for certain boundary conditions of an infinite solid, namely when temperature at infinity is constant and deformation there is zero. They show further that the heat-diffusion equation is valid with a diffusion constant containing the effective specific heat $((1 + \sigma)c_p + 2((1 - 2\sigma)c_V) / (3(1 - \sigma)))$, where σ is the isothermal Poisson ratio. Inserting $\sigma = (3K_T - 2G) / (6K_T + 2G)$ one readily finds that the effective specific heat is c_l . The longitudinal specific heat also appeared in Biot's 1956 paper [7] in his diffusion equation for the entropy density. Although not very different from c_p , there is a fundamental difference, and c_l pops up in many thermoelastic problems when they are treated exactly. In particular, as we have seen in this paper, there is only a cooling-by-heating effect if $c_l \neq c_p$. We originally proposed

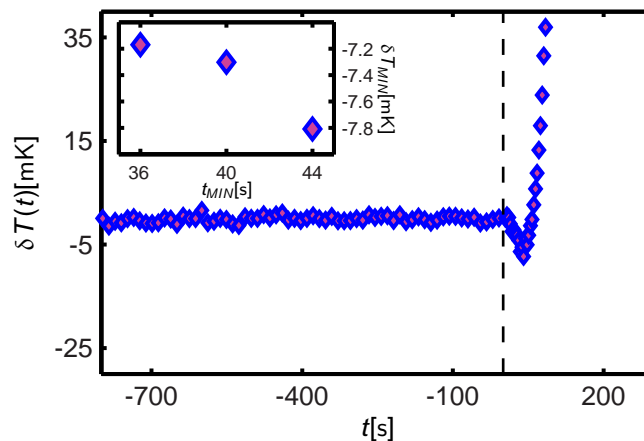


FIG. 12: The temperature in the center of a sphere of glucose, with diameter 19mm. At time $t = 0$ s a step in temperature from 298K to 303K is made with the cryostat (see the setup in Fig. 11). The temperature drops initially by 7.3mK as result of cooling-by-heating. The inset shows the minimum temperature δT_{MIN} reached in three measurements, on three different samples, at the same temperature.

the name longitudinal specific heat because this is the heat needed to increase temperature by 1 K if the associated expansion is confined to be longitudinal instead of isotropic.

Transient thermal stresses induced by surface heating of a sphere have been considered theoretically by Cheung *et al.* [24]. Their interest was fragmentation of brittle solids by surface heating. A heat current was applied uniformly within the polar angle regime $0 \leq \theta \leq \theta_0$ and the temperature and stress distributions calculated in time and space. This is a problem very similar to the one considered in this paper, although not generalized to situations with relaxation. However the cooling-by-heating phenomenon was not seen, since the standard decoupled heat-diffusion equation was used. The phenomenon thus seems apparently not to have been recognized in the literature, even though it belongs to classical continuum physics.

Other kinds of phenomena have lately been termed by the phrase “cooling-by-heating” or related names. Thus in 1999 Aleshin *et al.* reported “heating through cooling” when a copper bar is first heated to 150 °C and subsequently rapidly cooled. This result in a temperature increase at the other end of the bar of about 4°C [25]. The authors presented the following explanation: The sudden cooling causes the bar to contract, producing an elastic wave that propagates towards the cold end of the bar. Under certain conditions this wave triggers a sequence of events responsible for an energy release, similar to a process called a “steam explosion” in an ionic liquid which is observed when a water jet interacts with a molten salt, an explosion that does not take place where the water hits the molten salt, but at the bottom of the container [26]. In 2007 Zwickl *et al.* reported a “counter-intuitive cooling-by-heating” effect for laser cooling of a microcantilever, an observation they suggested is due to photothermal forces causing the lowest cantilever vibrational mode to cool while all other modes are heated [27]. Very recently Mari and Eisert discussed theoretically cooling of quantum systems by means of incoherent thermal light [28]. While coherent driving of a quantum system can mimic the effect of a cold thermal bath, the novel idea is that under certain conditions even incoherent “thermal” light can be used to cool a quantum system.

VII. SUMMARY

We have shown that cooling by heating occurs at the center of a solid spherical sample if it is heated at a mechanically free surface, reflecting a non-trivial thermomechanical coupling where the temperature initially decreases in the interior of the sphere. What happens is that, as heat diffuses into the outermost parts of the sphere, these parts expand and build up a negative pressure at the center of the sphere. This negative pressure couples to the temperature via the adiabatic pressure coefficient $\left(\frac{\partial T}{\partial p}\right)_S$. The opposite effect also applies, of course: if the temperature of the surface is lowered, heating by cooling will be observed. In ordinary solids the cooling-by-heating effect is almost negligible because their thermal expansion is generally small. The effect is particularly large for liquids close to their glass transition. The cooling-by-heating phenomenon establishes the difference between the longitudinal and isobaric specific heat, since the effect is only present when these two quantities differ. This is the case when the shear modulus is non-vanishing compared to the bulk modulus and, simultaneously, the isobaric and isochoric specific heats differ significantly. Analytical results show that the phenomenon occurs in the elastic case (the solid), and numerical results based on a model of the glass transition with parameters determined by glucose data show that the effect is present dynamically also in the very viscous liquid. Even in the hypothetical case when the glassy state is assumed to have zero expansivity, the phenomenon still appears at the glass transition.

The numerical results based on glucose data indicate that the drop in temperature at the center of the sphere is of order 5 mK with a duration of approximately 15 seconds when the temperature is increased by 1K on the surface of a sphere of radius $r = 10$ mm. This prediction was confirmed experimentally.

Acknowledgments

This work grew out of a suggestion by Niels Boye Olsen to whom we are obviously indebted. The center for viscous liquid dynamics ‘‘Glass and Time’’ is sponsored by The Danish National Research Foundation.

Appendix

1. Solution from section III - the transfer matrix method

The solution to the problem given in section III is based on the transfer matrix formulation [1, 2, 29] of the general solution of the thermoviscoelastic problem in a spherically symmetric case. Including the radial stress field and the time-integrated heat-current density that relate to the temperature and displacement fields, the authors of Refs. 1, 2 end up with four coupled equations to solve. Laplace transforming the equations relating the four fields and solving the resulting inhomogeneous system of four ordinary differential equations, the result is in the general form of a transfer matrix $\tilde{\mathbf{T}}(j, i)$ that links the dimensionless complex amplitudes of the fields at the boundary r_i with those at r_j :

$$\begin{pmatrix} \delta\tilde{p}_r \\ \delta\tilde{T} \\ \delta\tilde{V} \\ \delta\tilde{S} \end{pmatrix}_j = \tilde{\mathbf{T}}(j, i) \begin{pmatrix} \delta\tilde{p}_r \\ \delta\tilde{T} \\ \delta\tilde{V} \\ \delta\tilde{S} \end{pmatrix}_i. \quad (\text{A55})$$

Here $\delta\tilde{S}$, $\delta\tilde{V}$, $\delta\tilde{T}$, and $\delta\tilde{p}_r$ are the complex amplitudes of entropy, volume, temperature, and the radial component of pressure ($\delta\tilde{p}_r = -\tilde{\sigma}_{rr}$), respectively. The elements of the transfer matrix are given in reference [2]. From this general solution one can work out different cases, like the ones in Sec. III. The boundary condition at $\tilde{r}_1 = 0$, giving net flux of heat through the center of the sphere, was set equal to zero, $\delta\tilde{S}_1 = 0$, since heat is supplied uniformly across the surface \tilde{r}_3 giving a spherically symmetric case. For the same reason, $\delta\tilde{V}_1 = 0$. At the mechanically free outer boundary \tilde{r}_3 the heat supplied, $\delta\tilde{S}_3$, is given and $\delta\tilde{p}_{r,3} = 0$. Letting $\tilde{r} = \tilde{r}_2$ be an intermediate variable radius between \tilde{r}_1 and \tilde{r}_3 one has

$$\begin{pmatrix} \delta\tilde{p}_r \\ \delta\tilde{T} \\ \delta\tilde{V} \\ \delta\tilde{S} \end{pmatrix}_2 = \tilde{\mathbf{T}}(2, 1) \begin{pmatrix} \delta\tilde{p}_r \\ \delta\tilde{T} \\ 0 \\ 0 \end{pmatrix}_1. \quad (\text{A56})$$

Also

$$\begin{pmatrix} 0 \\ \delta\tilde{T} \\ \delta\tilde{V} \\ \delta\tilde{S} \end{pmatrix}_3 = \tilde{\mathbf{T}}(3, 1) \begin{pmatrix} \delta\tilde{p}_r \\ \delta\tilde{T} \\ 0 \\ 0 \end{pmatrix}_1. \quad (\text{A57})$$

This leads to $\delta\tilde{p}_{r,1} = -\frac{\tilde{T}_{12}(3,1)}{\tilde{T}_{11}(3,1)}\delta\tilde{T}_1$, or $\delta\tilde{T}_1 = -\frac{\tilde{T}_{11}(3,1)}{\tilde{T}_{12}(3,1)}\delta\tilde{p}_{r,1}$ whereby $\delta\tilde{S}_3 = (\tilde{T}_{42}(3, 1) - \frac{\tilde{T}_{41}(3,1)\tilde{T}_{12}(3,1)}{\tilde{T}_{11}(3,1)})\delta\tilde{T}_1 = (\tilde{T}_{41}(3, 1) - \frac{\tilde{T}_{42}(3,1)\tilde{T}_{11}(3,1)}{\tilde{T}_{12}(3,1)})\delta\tilde{p}_{r,1}$.

This implies

$$\delta\tilde{T}_1 = \frac{-\tilde{T}_{11}(3, 1)}{\tilde{T}_{41}(3, 1)\tilde{T}_{12}(3, 1) - \tilde{T}_{42}(3, 1)\tilde{T}_{11}(3, 1)}\delta\tilde{S}_3 \quad (\text{A58})$$

$$\delta\tilde{p}_{r,1} = \frac{\tilde{T}_{12}(3, 1)}{\tilde{T}_{41}(3, 1)\tilde{T}_{12}(3, 1) - \tilde{T}_{42}(3, 1)\tilde{T}_{11}(3, 1)}\delta\tilde{S}_3. \quad (\text{A59})$$

Inserting this into Eq. (A56) one has

$$\delta\tilde{p}_r(\tilde{r}) = \delta\tilde{p}_{r,2} = \frac{\tilde{T}_{11}(2,1)\tilde{T}_{12}(3,1) - \tilde{T}_{12}(2,1)\tilde{T}_{11}(3,1)}{\tilde{T}_{41}(3,1)\tilde{T}_{12}(3,1) - \tilde{T}_{42}(3,1)\tilde{T}_{11}(3,1)}\delta\tilde{S}_3 \quad (\text{A60})$$

$$\delta\tilde{T}(\tilde{r}) = \delta\tilde{T}_2 = \frac{\tilde{T}_{21}(2,1)\tilde{T}_{12}(3,1) - \tilde{T}_{22}(2,1)\tilde{T}_{11}(3,1)}{\tilde{T}_{41}(3,1)\tilde{T}_{12}(3,1) - \tilde{T}_{42}(3,1)\tilde{T}_{11}(3,1)}\delta\tilde{S}_3 \quad (\text{A61})$$

$$\delta\tilde{V}(\tilde{r}) = \delta\tilde{V}_2 = \frac{\tilde{T}_{31}(2,1)\tilde{T}_{12}(3,1) - \tilde{T}_{32}(2,1)\tilde{T}_{11}(3,1)}{\tilde{T}_{41}(3,1)\tilde{T}_{12}(3,1) - \tilde{T}_{42}(3,1)\tilde{T}_{11}(3,1)}\delta\tilde{S}_3 \quad (\text{A62})$$

$$\delta\tilde{S}(\tilde{r}) = \delta\tilde{S}_2 = \frac{\tilde{T}_{41}(2,1)\tilde{T}_{12}(3,1) - \tilde{T}_{42}(2,1)\tilde{T}_{11}(3,1)}{\tilde{T}_{41}(3,1)\tilde{T}_{12}(3,1) - \tilde{T}_{42}(3,1)\tilde{T}_{11}(3,1)}\delta\tilde{S}_3. \quad (\text{A63})$$

Inserting the actual explicit values of the transfer matrix elements from [2] and evaluating them in the limit of $\tilde{r}_1 \rightarrow 0$, putting $\tilde{r} = \tilde{r}_2$ $\tilde{R} = \tilde{r}_3$, yields

$$\delta\tilde{p}_r(\tilde{r}) = \frac{3\tilde{\alpha}\tilde{g}}{\tilde{c}(1+\tilde{g})} \left[\frac{1}{\tilde{R}^3} - \frac{\tilde{r} \cosh(\tilde{r}) - \sinh(\tilde{r})}{\tilde{r}^3(\tilde{R} \cosh(\tilde{R}) - \sinh(\tilde{R}))} \right] \delta\tilde{S}(\tilde{R}) \quad (\text{A64})$$

$$\delta\tilde{T}(\tilde{r}) = \frac{1}{\tilde{c}} \left[\frac{1}{\tilde{R}^3} \frac{3\tilde{\alpha}^2\tilde{g}}{\tilde{\alpha}^2\tilde{g} + \tilde{c}(1+\tilde{g})} - \frac{\sinh(\tilde{r})}{\tilde{r}(\tilde{R} \cosh(\tilde{R}) - \sinh(\tilde{R}))} \right] \delta\tilde{S}(\tilde{R}) \quad (\text{A65})$$

$$\delta\tilde{V}(\tilde{r}) = \frac{\tilde{\alpha}}{\tilde{c}(1+\tilde{g})} \left[\left(\frac{\tilde{r}}{\tilde{R}} \right)^3 \frac{\tilde{g}(\tilde{\alpha}^2 - \tilde{c}(1+\tilde{g}))}{\tilde{\alpha}^2\tilde{g} + \tilde{c}(1+\tilde{g})} - \frac{\tilde{r} \cosh(\tilde{r}) - \sinh(\tilde{r})}{\tilde{R} \cosh(\tilde{R}) - \sinh(\tilde{R})} \right] \delta\tilde{S}(\tilde{R}) \quad (\text{A66})$$

$$\delta\tilde{S}(\tilde{r}) = \frac{\tilde{r} \cosh(\tilde{r}) - \sinh(\tilde{r})}{\tilde{R} \cosh(\tilde{R}) - \sinh(\tilde{R})} \delta\tilde{S}(\tilde{R}). \quad (\text{A67})$$

The transformation back to dimensionalized physical quantities is performed by noticing that $\tilde{r} = kr$, $\tilde{R} = kR$, $\tilde{u} = ku$, where $k = \sqrt{sc_l/\lambda}$. Furthermore $\tilde{c} = T_0c_l/K_T$, $\tilde{\alpha} = T_0\alpha_p$, $\tilde{g} = 4G/(3K_T)$, $\tilde{\sigma}_{rr} = \sigma_{rr}/K_T$, $\delta\tilde{V} = \delta V k^3/(4\pi)$, $\delta\tilde{S} = \delta S k^3/(4\pi K_T)$, $\delta\tilde{T} = \delta T/T_0$. Since the entropy-displacement is positive in the direction of r , it is related to the heat input at the outer surface by $\delta Q = -T_0\delta S$, opposite of the convention in Ref. 2. Recalling that $\tilde{u} = \tilde{r}^2\tilde{V}$ one now easily derives Eqs. (24) and (25) from Eqs. (A65) and (A66).

2. Inverse Laplace-Stieltjes transforms.

If a stimulus $\phi_s e^{st}$ ($s = i\omega$) on a linear system gives rise to a response $\gamma_s e^{st}$, where $\gamma_s = f(s)\phi_s$, the response to a Heaviside input $\phi_0 H(t)$ will be $\gamma(t) = F(t)\phi_0$, where $F(t)$ is the inverse Laplace transform of $f(s)/s$ (or the inverse Laplace-Stieltjes transform of $f(s)$). We perform the inverse Laplace transform via the calculus of residues as

$$F(t) = \sum_{\text{poles } s_n} \text{Res}\left(\frac{f(s)}{s}, s_n\right) e^{s_n t} \quad (\text{A68})$$

Put $\rho = r/R$ and $\tau = (c_l/\lambda)R^2$. Then $kr = \sqrt{s\tau}\rho$. Choose furthermore initially time units such that $\tau = 1$. Then the two expressions of Eqs. (21) and (22) when divided by s become

$$\frac{f_1(s)}{s} = \frac{\sinh(\rho\sqrt{s})}{3\rho\sqrt{s}} \frac{\sqrt{s}}{\sqrt{s} \cosh(\sqrt{s}) - \sinh(\sqrt{s})} \quad (\text{A69})$$

$$\frac{f_2(s)}{s} = \frac{1}{\rho^3 s} \frac{\rho\sqrt{s} \cosh(\rho\sqrt{s}) - \sinh(\rho\sqrt{s})}{\sqrt{s} \cosh(\sqrt{s}) - \sinh(\sqrt{s})}. \quad (\text{A70})$$

Both expressions have simple poles at $s = 0$ with residue 1. The other poles are on the negative real axis $s_n = -x_n^2$, where x_n are the positive roots of the transcendental equation $\tan(x) = x$. $x_1 \approx 4.493409457$ and $x_2 \approx 7.725251836$ and $x_n \approx$

$\sqrt{(\pi/2 + n\pi)^2 - 2}$ better than 1 ppm for $n \geq 3$. The residues now become, respectively

$$\text{Res}\left(\frac{f_1(s)}{s}, -x_n^2\right) = \frac{2 \sin(\rho x_n)}{3\rho \sin(x_n)} \quad (\text{A71})$$

$$\text{Res}\left(\frac{f_2(s)}{s}, -x_n^2\right) = \frac{2 \sin(\rho x_n) - \rho x_n \cos(\rho x_n)}{\rho^3 x_n^2 \sin(x_n)}, \quad (\text{A72})$$

and the corresponding time-domain functions

$$F_1(\rho, t) = 1 + \frac{2}{3} \frac{1}{\rho} \sum_{n=1}^{\infty} \frac{\sin(\rho x_n)}{\sin(x_n)} e^{-x_n^2 t} \quad (\text{A73})$$

$$F_2(\rho, t) = 1 + 2 \left(\frac{1}{\rho}\right)^3 \sum_{n=1}^{\infty} \frac{\sin(\rho x_n) - \rho x_n \cos(\rho x_n)}{x_n^2 \sin(x_n)} e^{-x_n^2 t} \quad (\text{A74})$$

Using these expressions and reintroducing the characteristic heat diffusion time τ , one derives Eqs. (32), (33), and (34).

-
- [1] T. Christensen, N.B. Olsen, and J.C. Dyre, *Conventional methods fail to measure $c_p(\omega)$ of glass-forming liquids*, Phys. Rev. E **75**, 041502 (2007).
- [2] T. Christensen and J.C. Dyre, *Solution of the spherically symmetric linear thermoviscoelastic problem in the inertia-free limit*, Phys. Rev. E **78**, 021501 (2008).
- [3] G.S. Parks, H.M. Huffmann and F.R. Cattoir, *Studies on glass II. The transition between the glassy and liquid states in the case of glucose*, J. Phys. Chem **32**, 1366 (1928).
- [4] R.O. Davies and G.O. Jones, *The Irreversible Approach To Equilibrium In Glasses*, Proc. Roy. Soc.(London) **217**, 26-42 (1953).
- [5] H.H. Meyer and J.D. Ferry, *Viscoelastic Properties of Glucose Glass near Its Transition Temperature*, Trans. Soc. Rheol. **9**, 343-350 (1965).
- [6] R.M. Christensen, *Theory of Viscoelasticity*, (Academic, New York, 1982), 2nd ed.
- [7] M.A. Biot, *Thermoelasticity and Irreversible Thermodynamics.*, J. Appl. Phys. **27**, 240 (1956).
- [8] J.M.C. Duhamel, *Second mémoire sur les phénomènes thermo-mécaniques. J. de l'École Polytechnique*, **15**, 1 (1837).
- [9] W. Nowacki, *Thermoelasticity*, (Pergamon, London, 1986), 2nd ed.
- [10] H. Parkus. *Thermoelasticity*, (Springer-Verlag, Wien, 1976), 2nd ed.
- [11] P. Chadwick. *Thermoelasticity. The Dynamical Theory. Ch. VI in Progress in Solid Mechanics, Vol I edited by I. N. Sneddon and R. Hill.* (1960).
- [12] I.N. Sneddon. *The linear theory of thermoelasticity*, (Springer, Udine 1972).
- [13] R.B. Hetnarski and M.R. Eslami. *Thermal Stresses - Advanced Theory and Applications*, (Solid Mechanics and its applications Vol. 158, editor G. M. L. Gladwell, Springer 2009)
- [14] M. Lessen, *Thermoelasticity and Thermal Shock.*, J. Mech. Phys. Solids **5**, 57 (1956).
- [15] N.L. Ellegaard, T. Christensen, P.V. Christiansen, N.B. Olsen, U.R. Pedersen, T.B. Schrøder and J.C. Dyre, *Single-Order-Parameter Description of Glass-forming Liquids: A One-frequency Test*, J. Chem. Phys. **126**, 074502 (2007).
- [16] E.S. Greene, G.S. Parks, *The Thermal Conductivity of Glassy and Liquid Glucose*, J. Chem. Phys. **9**, 262 (1941)
- [17] G.S. Parks, L.E. Barton, M.E. Spaght and J.W. Richardson, *The Viscosity of Undercooled Liquid Glucose*, Physics **5**, 193 (1934)
- [18] B. Jakobsen, T. Hecksher, T. Christensen, N.B. Olsen, J.C. Dyre and K. Niss, *Communication: Identical Temperature Dependence of the Time Scales of Several Linear-Response Functions of two Glass-Forming Liquids*, J. Chem. Phys. **136**, 081102 (2012).
- [19] F.R. de Hoog, J.H. Knight, and A.N. Stokes, *An Improved Method for Numerical Inversion of Laplace Transforms*, SIAM. J. Sci. and Stat. Comput. **3**, 357 (1982).
- [20] K.J. Hollenbeck, *INVLAP.M: A matlab function for numerical inversion of Laplace transforms by the de Hoog algorithm* (2011); url: <http://www.isva.dtu.dk/staff/karl/invlap.htm>.
- [21] N.O. Birge and S.R. Nagel, *Specific-Heat Spectroscopy of the Glass Transition*, Phys. Rev. Lett. **54**, 2674 (1985)
- [22] B. Jakobsen, N.B. Olsen and T. Christensen, *Frequency-Dependent Specific Heat from Thermal Effusion in Spherical Geometry*, Phys. Rev. E **81**, 021503 (2010)
- [23] L.D. Landau and E.M. Lifshitz, *Theory of Elasticity*, (Pergamon, London, 1986), 3rd ed.
- [24] J.B. Cheung, T.S. Chen and K. Thirumalai, *Transient Thermal Stresses in a Sphere by Local Heating*, ASME J. Appl. Mech. **41**, 930 (1974).
- [25] G. Ya. Aleshin, J.C. Mollendorf, and J.D. Felske, *The Temperature Response of a Metallic Rod Near a "Steam Explosion"*, Int. Comm. Heat Mass Transfer **26**, 509 (1999).
- [26] G. Ya. Aleshin, *New Working Hypothesis of the "Steam-Explosion" Phenomenon*, Int. Comm. Heat Mass Transfer **24**, 497 (1997).
- [27] B. Zwickl, A. Jayich, and J.G.E. Harris, *Laser Cooling of a Microcantilever Using a Medium Finesse Optical Cavity*, paper presented at the Quantum Electronics and Laser Science Conference (QELS) (Baltimore, Maryland, May 6, 2007).
- [28] A. Mari and J. Eisert, *Cooling by Heating: Very Hot Thermal Light Can Significantly Cool Quantum Systems*, Phys. Rev. Lett. **108**, 12062 (2012).

[29] H.S. Carslaw and J.C. Jaeger, *Conduction of heat in Solids* (Clarendon Press, Oxford, 1959)